COMMUNICATION

OBC
www.rsc.org/obc

Limitations on the use of UV/Vis spectroscopy for the evaluation of conjugation effectiveness†

Nicolle N. P. Moonen and François Diederich*
Laboratorium für Organische Chemie, ETH-Hönggerberg, HCI, CH-8093, Zürich, Switzerland.
E-mail: diederich@org.chem.ethz.ch

Received 27th May 2004, Accepted 30th June 2004
First published as an Advance Article on the web 19th July 2004

A detailed study on *N*,*N*-dimethylanilino donor-substituted cyanoethynylethenes shows that there is no correlation between the effectiveness of the donor–acceptor conjugation pathway and the lowest-energy transition in the UV/Vis absorption spectrum.

Donor (D) – acceptor (A) interactions are often studied by UV/Vis spectroscopy. Intensive charge-transfer (CT) bands in the absorption spectra indicate strong D–A interactions. Furthermore, a more efficient conjugation pathway generally leads to a bathochromic shift of the lowest-energy transition band.

Here we describe the remarkable finding that in the case of the donor-substituted cyanoethynylethenes (CEEs)[1] the interpretation of the UV/Vis spectra (Fig. 1) will give misleading indications on the effectiveness of the conjugation pathways. The constitutional isomers **1a**–**3a** (Fig. 2) feature almost identical spectra in $CHCl_3$, with CEE **1a** having a longest-wavelength absorption maximum λ_{max} of 464 nm (2.67 eV),[2] **2a** of 467 nm (2.65 eV)[2] and **3a**‡ of 470 nm (2.64 eV). This similarity was not expected, since it is well established that cross-conjugation is less efficient than linear conjugation, which is normally reflected by a hypsochromic shift in the UV/Vis spectrum.[3] In contrast, the UV/Vis spectra (Fig. 1 of ESI†) of *N*,*N*-dimethylanilino (DMA) donor – *p*-nitrophenyl acceptor-substituted TEEs **6a**–**8a** in $CHCl_3$ (Fig. 2)[4] show the expected differences between cross-conjugated and linear conjugated compounds. The lowest-energy absorption of D–A cross-conjugated **8a** (λ_{max} = 447 nm, 2.77 eV) is hypsochromically shifted compared to those of linearly conjugated **6a** (λ_{max} = 471 nm, 2.63 eV) and **7a** (λ_{max} = 468 nm, 2.65 eV).

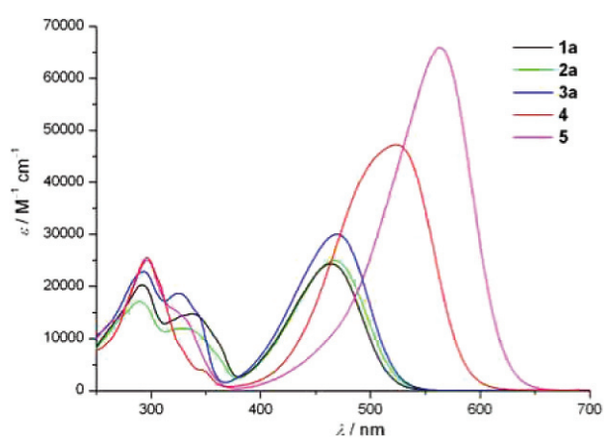

Fig. 1 UV/Vis spectra of **1a**–**3a**, **4** and **5** in $CHCl_3$ (for structures, see Fig. 2).

In order to obtain more insight into the different conjugation pathways of DMA donor-substituted CEEs and to find an explanation for the unusual features observed in their UV/Vis spectra, we carried out density functional calculations at the B3LYP[5] level of theory, which we present here.

The results of the geometry optimisations[6] of CEEs **1b**–**3b**, **4** and **5** (Fig. 2) with the B3LYP/6–31G** method are summarised in Table 1. All silyl protecting groups were replaced by hydrogens to save calculation time. Deprotection of the silyl groups in the TEEs resulted in a negligible shift in the UV/Vis spectra,[7] indicating only small electronic differences between the silyl-protected and deprotected compounds. The deprotected CEEs **1b**, **2b** and **3b** can therefore be seen as models for **1a**, **2a** and **3a**, respectively. Since an X-ray crystal structure of **5** was available,[1] the experimentally determined bond lengths could be compared with the calculated ones. The calculated and experimental bond lengths follow the same trends, validating[8] the calculation. The B3LYP calculation was performed without symmetry constraints. The fact that the short bonds are lengthened and the long bonds are shortened is consistent with the fact that DFT tends to favour delocalisation.

The bond length alternation in the DMA rings is a good indication of the amount of charge-transfer (CT) from the DMA donor to the CEE acceptor moiety, which can be expressed by the quinoid character δ*r* of the aryl ring (for definition,[9] see footnote to Table 1). In benzene, the δ*r* value equals 0, whereas values between 0.08 and 0.10 are found in fully quinoid rings. Within the series studied here, the highest quinoid value is obtained for bis-DMA-substituted CEE **4** (0.0320). The highest amount of CT and therefore conjugation for **4** can also be concluded from the ^{13}C NMR spectra. The downfield shifts of the aryl carbons *ipso* and *meta* to the Me_2N group indicate the removal of electron density from the DMA units (see Table 1 of ESI†). The δ*r* values of the donor–acceptor substituted TEEs,[4] calculated from several X-ray structures, generally do not exceed 0.025. This shows that DMA-substituted CEEs are much stronger CT chromophores than their TEE analogues.

The comparison between the three constitutional isomers **1b**, **2b** and **3b** is interesting. *Cis* D–A-substituted **2b** shows the highest amount of CT in the ground state, followed by the *trans* D–A isomer **1b** and the geminally substituted CEE **3b** (δ*r* = 0.0318, 0.0314 and 0.0309, respectively). This order could also be arrived at by the analysis of the ^{13}C NMR spectra of their Pr^i_3Si-protected analogues **1a**–**3a** (see Table 1 of ESI†).

The comparison of isomers **4** and **5** shows two *cis* and two *trans* D–A pathways for **4** and two geminal and two *cis* D–A pathways for **5**. Considering that cross-conjugation is less effective than linear conjugation, a larger δ*r* is expected and indeed calculated for **4**. The general rule that more efficient delocalisation results in a more stable molecule is confirmed: within the series **1b**–**3b**, the most conjugated molecule **2b** is 0.47 kcal mol^{-1} more stable than **1b**, which is 0.29 kcal mol^{-1} lower in energy than **3b**. Furthermore, the calculations show that **4** is 0.98 kcal mol^{-1} more stable than **5**. We are aware that some of these energy differences may be at the limit of significance at the DFT level.

A validation study for the electronic transition analysis by time-dependent DFT calculations (TDFT) with different functionals was carried out on **5**. The local density approximation SVWN5[10] and the BP86[11] functionals with a 6–31G* basis set gave similar transitions, which were approximately 0.40 eV too low in energy. Because the B3LYP functional gave a value that deviated by only 0.10 eV from the experimental data in hexane (λ_{max} = 524 nm, 2.37 eV, calculated

† Electronic supplementary information (ESI) available: UV/Vis spectra of **6a**–**8a** in $CHCl_3$, charge alternation plot for linear and cross-conjugation, selected ^{13}C-NMR and calculation data for **1a**–**3a**, **4** and **5**. See http://www.rsc.org/suppdata/ob/b4/b407940j/

DOI: 10.1039/b407940j

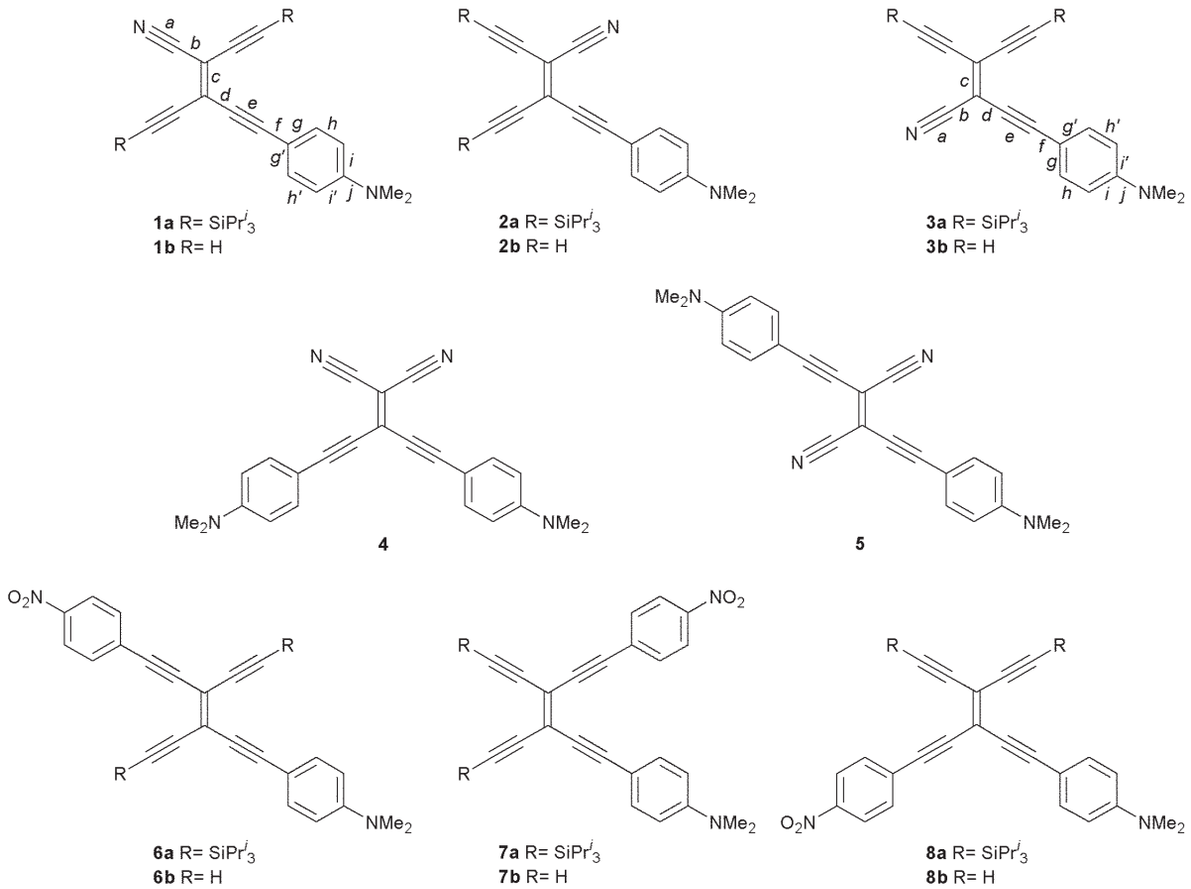

Fig. 2 *N,N*-dimethylanilino donor-substituted CEEs and TEEs with definition of bond lengths.

Table 1 Calculated bond lengths in Å of donor-substituted CEEs, using the B3LYP/6–31G** method. For bond length definitions, see Fig. 2

	a	*b*	*c*	*d*	*e*	*f*	(*g* + *g*′)/2	(*h* + *h*′)/2	(*i* + *i*′)/2	*j*	δ*r*[a]
1b	1.164	1.430	1.389	1.410	1.222	1.414	1.4118	1.3842	1.4194	1.376	0.0314
2b	1.164	1.431	1.390	1.409	1.222	1.413	1.4120	1.3840	1.4196	1.376	0.0318
3b	1.163	1.436	1.388	1.408	1.222	1.414	1.4117	1.3845	1.4191	1.377	0.0309
4	1.165	1.424	1.399	1.410	1.222	1.413	1.4121	1.3839	1.4197	1.376	0.0320
5[b]	1.163	1.434	1.394	1.404	1.223	1.413	1.4121	1.3842	1.4193	1.377	0.0315
	1.146	1.441	1.372	1.417	1.207	1.422	1.399	1.372	1.411	1.368	0.033

[a] δ*r* = (((*g* + *g*′)/2 − (*h* + *h*′)/2) + ((*i* + *i*′)/2 − (*h* + *h*′)/2))/2. [b] For **5**, the upper data set corresponds to the calculated bond lengths, the lower set to the X-ray crystal data.[1]

Table 2 Calculated orbital energies in eV, relative to E(HOMO) of **1b** (absolute value: −5.339 eV), based on the B3LYP/6–31G** method

Compound	*E*(HOMO-1)	*E*(HOMO)	*E*(LUMO)	Δ*E*(L − H)	Δ*E*(L − (H − 1))
1b	−1.020	0	+2.886	2.886	3.906
2b	−0.998	+0.091	+2.910	2.819	3.908
3b	−1.075	+0.104	+2.884	2.788	3.959
4	−0.016	+0.032	+2.840	2.808	2.856
5	−0.024	+0.443	+2.801	2.358	2.825

2.27 eV, Table 2 of ESI†) and provided previously good results for the TEEs,[12] we decided to use this functional for our analysis.

The calculated transitions of the mono-donor substituted CEE isomers **1b**, **2b** and **3b** are in excellent agreement with the experimental UV/Vis data in hexane ($\Delta E_{gap} \leq 0.03$ eV, see Table 2 of ESI†). All lowest-energy transitions are mainly composed of a HOMO → LUMO transition. These calculated transitions show oscillator strengths *f* (0.8) and transition dipole moments *M* (8.5–8.7 Debye) that are higher than the values obtained from the UV/Vis spectra (*f* ~0.4, *M* ~6 Debye).[13] The second, less intense, higher-energy band is calculated to be located around 330 nm, which agrees with the experimental spectra. This band is in all cases mainly composed of a HOMO-1 → LUMO transition.

The energies of the LUMOs of the three isomers **1b**, **2b** and **3b** are very similar (within 0.026 eV, Table 2). At this point, it should be noted that the energies of the orbitals are based on ground state geometries and can therefore only be used for qualitative analyses. The similarity in the energies of the LUMOs is also apparent in their orbital shapes (Fig. 3), which all have the density concentrated on the CEE acceptor part. The differences in the energy of the HOMO levels are significantly larger (up to 0.104 eV). The HOMOs show CT from the DMA fragment to the CEE acceptor. The highest-energy HOMO (for **3b**) is probably due to the compound's less favourable geminal conjugation path. This cross-conjugated pathway contains one carbon less than the linear conjugation pathway. When the principle of charge alternation is considered, a very unfavourable partial positive charge is located on the nitrogen of the cyano group (see Fig. 2 in ESI†). CEE **2b** shows more CT in the ground state and is more stable than **1b**, but has a slightly higher-lying HOMO. The energy of the CT transition,

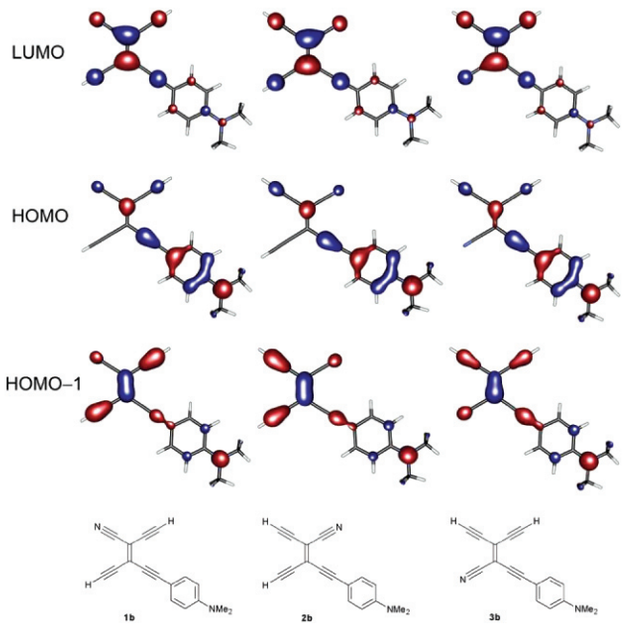

Fig. 3 Orbital plots of **1b**–**3b**, calculated from B3LYP/6–31G** optimised geometries.

being the lowest for **3b**, is mainly determined by the level of the HOMO.

At this stage, a comparison with the *p*-nitrophenyl-substituted TEEs **6b**–**8b** would be useful. Calculations on the INDO/S level[7,14] predicted that λ_{max} for the DMA donor – *p*-nitrophenyl acceptor-substituted TEEs would be the most red-shifted for *cis* isomer **7b**, followed by *trans* isomer **6b**, and then by geminal isomer **8b**. This order was indeed found in the UV/Vis spectra of the silyl-protected analogues **6a**–**8a** (*vide supra*). The cross-conjugated (geminally substituted) CEE **3b** and TEE **8b** are of special interest, since **3a** has the most red-shifted λ_{max} within the CEE series and **8a** the most blue-shifted λ_{max} within the TEE series. The lowest-energy absorptions of the TEEs are also mainly composed of a HOMO → LUMO transition.[7,14] The differences in the energies between the HOMOs and LUMOs of the three isomers **6b**–**8b** are very small (within 0.02–0.03 eV).[7] This can be explained by the HOMO and LUMO plots in Fig. 4. The HOMO shows partial CT from the DMA to the TEE core but *not* to the *p*-nitrophenyl-accepting unit. This causes identical-looking HOMOs, which are more or less independent of the D–A conjugation pathway. The density in the LUMOs is located on the TEE and the *p*-nitrophenyl group, again generating identical plots for the three isomers.

The TDFT calculations failed completely for the TEEs. They gave very complicated spectra that did not correspond to the experimentally found transitions. INDO/S calculations on the same optimised geometries (B3LYP/6–31G**) reproduced the previously published results.[7,14] This indicates that the failure of the TDFT method cannot be attributed to the optimised geometry.

The differences in the absorption spectra between the TEE and the CEE cross-conjugated systems can apparently be attributed to the nature of the electron-accepting group. The cyano group is in this case a stronger electron acceptor than the (*p*-nitrophenyl)ethynyl unit. The nitrile dominates the HOMO more than the *p*-nitrophenyl group, resulting in a larger destabilisation of the HOMO level of the geminally substituted CEE **3b** as compared to that of TEE **8b**.

By going from systems with one strong donor and one acceptor to CEEs with two donors and two acceptors, the situation becomes more complicated, since more conjugation pathways are involved (*vide supra*).

The TDFT calculation indicates that the lowest-energy band for **5** is composed of a HOMO → LUMO transition (Table 2 of ESI†), similar to the mono donor-substituted CEEs. For **4** this low-energy band consists of two separate bands, being a HOMO-1 → LUMO transition and a HOMO → LUMO transition. The LUMO levels are slightly lower than those of **1b**–**3b** (Table 2). This agrees with the results of the cyclic voltammetry measurements, with **4** and **5** being easier to reduce than **1a**–**3a**.[1] The largest energy differences are again located in the HOMO. The HOMO-1 and LUMO levels of **4** and **5** are almost equal in energy. The HOMO level of **5** is 0.41 eV higher in energy than that of **4**, which explains the lower transition energy of **5** (λ_{max} = 563 nm, 2.20 eV in $CHCl_3$, compared to λ_{max} = 524 nm, 2.37 eV for **4**).[1] The higher energy level of the HOMO of **5** correlates with the easier oxidation of this compound compared to **4**.[1] The HOMO plots (Fig. 5) reveal that the density in **5** is completely located on the donors and the double bond. In contrast, CT from the donor units to the cyano accepting groups is observed in the HOMO of **4**. The reason for the absence of CT in the HOMO of **5** is not understood, but it may be the reason for the higher energy of the HOMO of **5** compared to **4**. Charge-transfer from a donor to an acceptor generally leads to a lower energy (*vide supra*). Also in this case, the most conjugated molecule (**4**) does not show the most red-shifted λ_{max}. The same feature was also observed for the *p*-nitrophenyl-substituted TEE analogues of **4** and **5**.[4]

It can be concluded that TDFT can give results that are very close to the experimentally observed transitions. However, the method

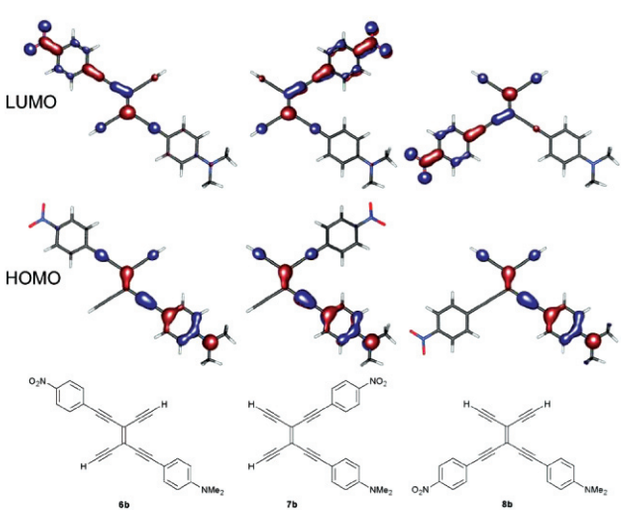

Fig. 4 Orbital plots of **6b**–**8b**, calculated from B3LYP/6–31G** optimised geometries.

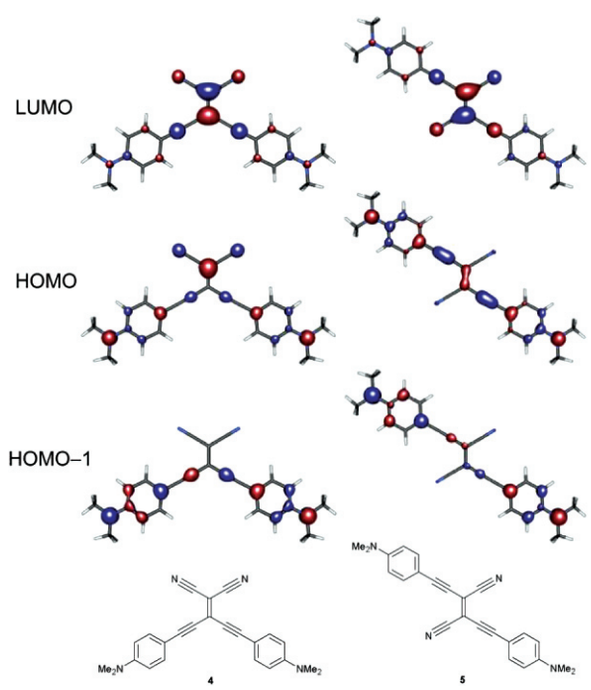

Fig. 5 Orbital plots of **4** and **5**, calculated from B3LYP/6–31G** optimised geometries.

can also fail severely as shown for the *p*-nitrophenyl-substituted TEEs. Therefore, the results of this method have to be critically evaluated and if possible compared to results of other methods such as INDO/S.

Within series of constitutional isomers of donor-substituted CEEs, the variance in the lowest-energy transitions is caused by the differences in the HOMO energy. By changing the electron-accepting group from nitrile in the CEEs to (*p*-nitrophenyl)ethynyl in the TEEs, the HOMO obtains less CT character and the HOMO of the cross-conjugated TEE (**8b**) is less destabilised. The nature of the electron-accepting substituent in the geminal position is obviously very important for the spectral properties of cross-conjugated compounds.

UV/Vis spectra are often used to evaluate the effectiveness of different conjugation pathways (*vide supra*), assuming that a more red-shifted λ_{max} results from a better conjugation. The examples in this paper show this correlation is not always valid. Similar conclusions were recently reached by *Meier et al.* in the study of donor-substituted oligo(*p*-phenyleneethylene)s[15] and oligo(*p*-phenylenevinylene)s.[16] Special care has to be taken with the interpretation of UV/Vis spectra of compounds with strong donors and acceptors. For these compounds, the λ_{max} in the UV/Vis spectrum should only be considered as a measure of the change of the degree of CT in the transition from the ground state to the excited state, and should not be used for the study of conjugation effectiveness. For the evaluation of the effectiveness of different conjugation pathways, methods describing the ground-state, such as thermochemistry, X-ray analysis, ^{13}C-NMR spectroscopy and ground state geometry and energy calculations, are much more suitable.

Acknowledgements

Support by the ETH Research Council and the German Fonds der Chemischen Industrie is gratefully acknowledged. Dr Christine Jamorski-Jödicke is thanked for the validation study.

Notes and references

‡ CEE **3a** was characterised by IR, UV/Vis, ^{1}H and ^{13}C NMR, and elemental analysis.

1 N. N. P. Moonen, R. Gist, C. Boudon, J. P. Gisselbrecht, P. Seiler, T. Kawai, A. Kishioka, M. Gross, M. Irie and F. Diederich, *Org. Biomol. Chem.*, 2003, **1**, 2032–2034.

2 Error in reference 1. The UV/Vis spectral data of **1a** (number **1** in ref. 1) and **2a** (number **2** in ref. 1) should be interchanged.

3 A. M. Boldi, J. Anthony, V. Gramlich, C. B. Knobler, C. Boudon, J. P. Gisselbrecht, M. Gross and F. Diederich, *Helv. Chim. Acta*, 1995, **78**, 779–796; R. R. Tykwinski and Y. Zhao, *Synlett*, 2002, 1939–1953; E. Burri, F. Diederich and M. B. Nielsen, *Helv. Chim. Acta*, 2001, **84**, 2169–2182.

4 R. R. Tykwinski, M. Schreiber, R. P. Carlón, F. Diederich and V. Gramlich, *Helv. Chim. Acta*, 1996, **79**, 2249–2281; R. R. Tykwinski, M. Schreiber, V. Gramlich, P. Seiler and F. Diederich, *Adv. Mater.*, 1996, **8**, 226–231.

5 A. D. Becke, *J. Chem. Phys.*, 1993, **98**, 5648–5652; C. Lee, W. Yang and R. G. Parr, *Phys. Rev. B*, 1988, **37**, 785–789.

6 All calculations were carried out in Gaussian 98, Revision A.7: M. J. Frisch, G. W. Trucks, H. B. Schlegel, G. E. Scuseria, M. A. Robb, J. R. Cheeseman, V. G. Zakrzewski, J. A. Montgomery, Jr., R. E. Stratmann, J. C. Burant, S. Dapprich, J. M. Millam, A. D. Daniels, K. N. Kudin, M. C. Strain, O. Farkas, J. Tomasi, V. Barone, M. Cossi, R. Cammi, B. Mennucci, C. Pomelli, C. Adamo, S. Clifford, J. Ochterski, G. A. Petersson, P. Y. Ayala, Q. Cui, K. Morokuma, D. K. Malick, A. D. Rabuck, K. Raghavachari, J. B. Foresman, J. Cioslowski, J. V. Ortiz, B. B. Stefanov, G. Liu, A. Liashenko, P. Piskorz, I. Komaromi, R. Gomperts, R. L. Martin, D. J. Fox, T. Keith, M. A. Al-Laham, C. Y. Peng, A. Nanayakkara, C. Gonzalez, M. Challacombe, P. M. W. Gill, B. G. Johnson, W. Chen, M. W. Wong, J. L. Andres, M. Head-Gordon, E. S. Replogle and J. A. Pople, *GAUSSIAN 98 (Revision A.7)*, Gaussian, Inc., Pittsburgh, PA, 1998.

7 A. Hilger, Dissertation ETH No. 12928, Zürich, 1998.

8 Hartree–Fock geometry optimisations give an underestimation of the quinoid character δ*r*, whereas B3LYP with the smaller basis set 3–21G resulted in an overestimation of δ*r*.

9 C. Dehu, F. Meyers and J.-L. Brédas, *J. Am. Chem. Soc.*, 1993, **115**, 6198–6206; A. Hilger, J.-P. Gisselbrecht, R. R. Tykwinski, C. Boudon, M. Schreiber, R. E. Martin, H. P. Lüthi, M. Gross and F. Diederich, *J. Am. Chem. Soc.*, 1997, **119**, 2069–2078.

10 J. C. Slater, *Phys. Rev.*, 1951, **81**, 385–390; S. H. Vosko, L. Wilk and M. Nusair, *Can. J. Phys.*, 1980, **58**, 1200–1211.

11 A. D. Becke, *Phys. Rev. A.*, 1988, **38**, 3098–3100; J. P. Perdew, *Phys. Rev. B*, 1986, **33**, 8822–8824.

12 L. Gobbi, N. Elmaci, H. P. Lüthi and F. Diederich, *ChemPhysChem*, 2001, **2**, 423–433.

13 N. N. P. Moonen, Dissertation ETH No. 15468, Zürich, 2004.

14 R. E. Martin, J. Bartek, F. Diederich, R. R. Tykwinski, E. C. Meister, A. Hilger and H. P. Lüthi, *J. Chem. Soc., Perkin Trans. 2*, 1998, 233–241.

15 H. Meier, B. Mühling and H. Kolshorn, *Eur. J. Org. Chem.*, 2004, 1033–1042.

16 H. Meier, J. Gerold, H. Kolshorn and B. Mühling, *Chem. Eur. J.*, 2004, **10**, 360–370.